Grafting of Polymers from Clay Nanoparticles via In Situ Free Radical Surface-Initiated Polymerization: Monocationic versus Bicationic Initiators

Xiaowu Fan,† Chuanjun Xia,† and Rigoberto C. Advincula*,†,‡

Materials Science Program and Department of Chemistry, University of Alabama at Birmingham, Birmingham, Alabama 35294-1240, and Department of Chemistry, University of Houston, Houston, Texas 77204-5003

Received November 8, 2002. In Final Form: January 31, 2003

Surface-initiated polymerization (SIP) from clay nanoparticles was compared between surface-bound mono- and bicationic free radical initiators. Distinct properties in molecular weight (MW), extent of exfoliation, and particle morphology were observed as a consequence of using two different initiator architectures. X-ray diffraction (XRD) results showed that the clay intercalated with monocationic initiator has a larger *d* spacing and gave a more ordered structure. IR, X-ray photoelectron spectroscopy, and qualitative thermogravimetric analysis confirmed the attachment of both initiators. XRD further showed that the SIP product from the bicationic initiator retained some intercalated structure while a highly exfoliated structure is achieved by the SIP through the monocationic initiator. Consequently the monocationic initiator gave a higher MW polymer. We have found that well-dispersed intercalated clay particles and efficient monomer diffusion are crucial factors in performing a successful SIP and in achieving an exfoliated clay structure.

Introduction

Polymer-layered silicate (PLS) nanocomposites have continuously attracted much interest since the first nylon-6−clay hybrid (NCH) materials were reported.[1,2] The interest in PLS nanocomposites can be attributed to improved mechanical, barrier, and heat-resistant properties over their pristine macrocomposite counterparts. There are two main types of PLS nanocomposite materials:[3] (1) *Intercalated*, in which polymer chains are inserted into the interlayer spacing of the stacking silicate platelets. The *d* spacing value of these well-ordered, polymer−silicate sandwich multilayers is greater than that of pristine clay. (2) *Delaminated/exfoliated*, in which the clay layers are uniformly and discretely dispersed in a continuous polymer matrix. Because of greater phase homogeneity with the latter, the delaminated structure is *more effective* in improving the properties of the polymer, especially at very low silicate loading. Thus, a delaminated PLS is practically more desirable than an intercalated one for nanocomposite materials.

There have been recent attempts to prepare PLS nanocomposites through an in situ intercalative polymerization approach. Pure clay is modified with either a monomer-cation or initiator-cation and then polymerized. This is because negatively charged layered clays, for example, montmorillonite aluminosilicate, possess exchangeable metal cations, such as Na^+, Li^+, Ca^{2+}, and so forth, at the spacing between layers. As a result, organic cations can be inserted into the interlayer galleries by an ion exchange process, forming inorganic clay−organic cation complexes, that is, *organophilic clay*. For example, intercalated polystyrene−clay nanocomposites have been synthesized by ion exchange with a vinylbenzylammonium cation and subsequent free radical polymerization of styrene with 2,2′-azobisisobutyronitrile (AIBN).[4,5] Through a similar method, Doh and Cho also reported the in situ polymerization of styrene with an organophilic clay in which PLS materials with an intercalated structure were also obtained.[6] Besides polystyrene−clay nanocomposites, poly(methyl methacrylate)−clay materials were also synthesized by in situ polymerization with the addition of lipophilized smectite clay. Different degrees of clay dispersion in the polymer matrix were obtained, and the result was studied in terms of effective organic cation intercalation and the types of monomer used.[7] Exfoliated polystyrene−clay nanocomposite materials were achieved from a solvent-free in situ free radical polymerization by Fu and Qutubuddin.[8] In their studies, organophilic clay was prepared by intercalation of a polymerizable cationic surfactant, which was then dispersed directly in monomer solution. Thus, all of these methods rely on lipophilizing clay and making it compatible to a typical free-radical polymerization.

Rather than modifying clay with organic quaternized ammonium salts, cationically modified polymerization initiators can also be used to prepare organophilic clays. In this method, in situ polymerization is initiated by activation of the initiators that are *ionically bound* to the clay particle surfaces, that is, through a surface-initiated polymerization (SIP) process. The advantage of SIP is based on the assumption that as the polymer chain grows after surface initiation, the ordered silicate layers could be gradually pushed apart, ultimately exfoliating to discrete laths, resulting in a well-dispersed structure of the final product. Also, theoretically, if all initiators are tethered to clay surfaces, a higher efficiency of intergallery

* To whom correspondence should be addressed.
† University of Alabama at Birmingham.
‡ University of Houston.

(1) Usuki, A.; Kojima, Y.; Kawasumi, M.; Okada, A.; Fukushima, Y.; Kurauchi T.; Kamigaito, O. *J. Mater. Res.* **1993**, *8*, 1179.
(2) Kojima, Y.; Usuki, A.; Kawasumi, M.; Okada, A.; Fukushima, Y.; Kurauchi, T.; Kamigaito, O. *J. Mater. Res.* **1993**, *8*, 1185.
(3) Burnside, S. D.; Giannelis, E. P. *Chem. Mater.* **1995**, *7*, 1597.
(4) Akelah, A.; Moet, A. *J. Mater. Sci.* **1996**, *31*, 3589.
(5) Moet, A.; Akelah, A. *Mater. Lett.* **1993**, *18*, 97.
(6) Doh, J. G.; Cho, I. *Polym. Bull.* **1998**, *41*, 511.
(7) Okamoto, M.; Morita, S.; Taguchi, H.; Kim, Y. H.; Kotaka, T.; Tateyama, H. *Polymer* **2000**, *41*, 3887.
(8) Fu, X.; Qutubuddin, S. *Polymer* **2001**, *42*, 807.

10.1021/la0268193 CCC: $25.00
Published on Web 04/09/2003

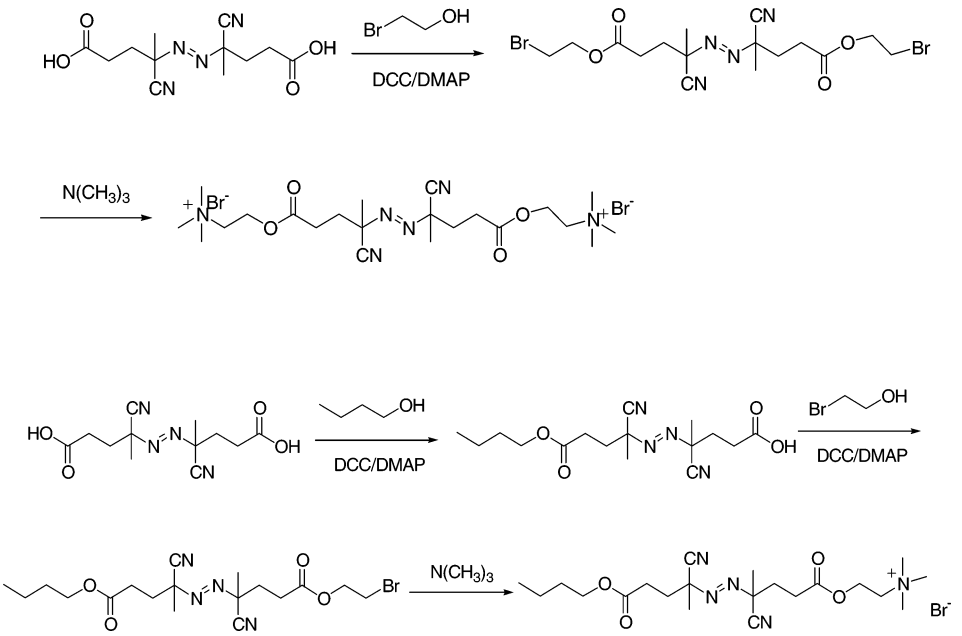

Figure 1. (a) Synthetic scheme and structure of the bicationic free radical initiator. (b) Synthetic scheme and structure of the monocationic free radical initiator.

polymerization is expected compared to that of free, unattached initiators. Exfoliated polystyrene−clay nanocomposites with controllable MW have been prepared by intercalating a charged living free radical polymerization (LFRP) initiator into montmorillonite.[9] Very recently, we have used a (1,1-diphenylethylene) DPE derivative initiator to synthesize polystyrene−clay nanocomposite materials through living anionic surface-initiated polymerization (LASIP).[10,11] However, only intercalated structures were obtained.

In our efforts to conduct SIP from clay surfaces, we recently synthesized two initiators for free radical SIP. They both have quaternized amine endgroups for cation exchange with montmorillonite particles. The initiator molecule design is as follows: (1) *symmetric*, with two cationic groups at both chain ends (named bicationic free radical initiator hereafter) and (2) *asymmetric*, with one cationic group at one end (named monocationic free radical initiator hereafter). The synthetic schemes and structures of these initiators are shown in Figure 1a,b. They are both AIBN-analogue initiators, useful for free radical polymerization. The use of another symmetric bicationic azo compound, 2,2′-azobis(isobutyramidine hydrochloride) (AIBA), has proven the feasibility of styrene SIP on high surface area mica powder.[12] However, no structural information for the SIP products was reported. Asymmetric azo initiators in the form of silanes have been successfully employed to free radically polymerize styrene from spherical silica gel surfaces.[13,14] To the best of our knowledge, there have been no reports on a *direct* free radical SIP approach from surface-bound monocationic azo initiators on individual clay nanoparticles.

In this paper, we report our comparative studies on the intercalation of two types of initiators into *partially exfoliated* montmorillonite clay nanoparticles and their nanocomposite products from free radical SIP. We have focused the study on differences in their structural characterization, exfoliation procedures, and MWs. This is in contrast to previous polymerization studies with unbound radical initiators and various organophilic clays.[8,12,26] In our case, the intercalation of our initiators provides both organophilicity for clay and the initiation functionality for the SIP process. Our work is also different from previous attempts to perform SIP directly on clay particles in which initiators are bound as organic layered silicates (OLSs) and polymerization is expected to result in exfoliation.[12,27,28] In our case, the goal is to investigate directly the grafting of polymers on clay nanoparticles where the polymers are expected to form a "shell" on the particle surface. Partial exfoliation of the platelets was achieved using a combined high rpm stirring and sonication process to separate clay into discrete platelets (several hundreds of nanometers in diameter), which retained a distribution of lamellar stacking (as shown by atomic force microscopy, Figure 9a). Overall, our goal is to understand the free radical SIP mechanism in confined environments and the effect of initiator design on the structure and composition of SIP products.

Experimental Section

Materials. Montmorillonite clay (commercially Cloisite Na^+) was provided by Southern Clay Products Inc. Deionized water used in all experiments was purified by a Milli-Q Academic system (Millipore Corp.) with a 0.22 micron Millistack filter at the outlet. Styrene monomer (Aldrich) was distilled at reduced pressure at room temperature before polymerization. All other reagents for the synthesis of the initiators and polymerization were purchased from Aldrich and used without further purification.

Initiator Synthesis. The synthesis routes of the two initiators are shown in Figure 1a,b. The synthesis of the symmetric free radical initiator involved the use of commercially available 4,4′-azobis(4-cyanovaleric acid) from Across. This acid was treated with bromoethanol by a well-known esterification method using DCC/DMAP[15] followed by stirring with an excess of trimethylamine in dry THF. The precipitate was collected and dried under vacuum. The asymmetric initiator was made in a similar way

(9) Weimer, M. W.; Chen, H.; Giannelis, E. P.; Sogah, D. Y. *J. Am. Chem. Soc.* **1999**, *121*, 1615.
(10) Zhou, Q.; Fan, X.; Xia, C.; Mays, J.; Advincula, R. *Chem. Mater.* **2001**, *13*, 2465.
(11) Fan, X.; Zhou, Q.; Xia, C.; Crsitopholi, W.; Mays, J.; Advincula, R. C. *Langmuir* **2002**, *18*, 4511.
(12) Meier, L.; Shelden, R.; Caseri, W.; Suter, U. *Macromolecules* **1994**, *27*, 1637.
(13) Pruker, O.; Ruhe, J. *Macromolecules* **1998**, *31*, 592.
(14) Pruker, O.; Ruhe, J. *Macromolecules* **1998**, *31*, 602.
(15) Neises, B.; Steglich, W. *Angew. Chem., Int. Ed.* **1978**, *17*, 522.

Table 1. Data Related to the Preparation of the Intercalated Clays

initiator	clay used (g)	theoretical initiator weight (g)	initiator actually added (g)	intercalated clay obtained (g)	yield
bicationic	1.3	0.366	0.45	1.35	87.5%
monocationic	1.3	0.600	0.74	1.57	88.4%

except that one end of the acid was blocked with a butanol group. Both products were analyzed by ^{1}H, ^{13}C NMR, and elemental analysis. The results showed that the target molecules were successfully synthesized (see Supporting Information). A manuscript containing detailed information about the initiator synthesis and characterization is under preparation.

Preparation of Initiator-Intercalated Clay Particles. The size and dimension (lateral, ca. hundreds of nanometers; thickness, ca. 1 nm) of clay particles in a homogenized suspension were in the form of partially exfoliated nanoplatelets (see Figure 9a). Nearly similar particle sizes and exfoliation methods have been used to prepare clay nanoparticles for the layer-by-layer preparation of nanocomposite ultrathin films with polyelectrolytes.[16,17] After ion exchange, the initiator is bound to the intergalleries of the clay lamellae (bicationic initiator) and the surface (monocationic initiator) of these nanoparticles. The term *intercalation* as used in the preparation of initiator-intercalated particles is then used in the context of using this type of particles. The preparation procedure is as follows:

Montmorillonite clay (1.3 g) (Table 1) was dispersed in 500 mL of deionized water, and the dispersion was stirred vigorously overnight at room temperature. The clay suspension was then ultrasonicated while stirring for 24 h, and a yellowish, homogeneous dispersion was obtained. Initiators were dissolved in deionized water to make 1.25 wt % aqueous solutions. By using the cation exchange capacity (CEC) value (92 mequiv/100 g) of the Cloisite Na^+ and the molecular weights of different initiators (502.45 g/mol for the monocationic initiator and 612.4 g/mol for the bicationic initiator), the exact weight (the weight of the initiator needed to fully replace the Na counterion of the clay used) of the two initiators was calculated. Accordingly, an excess amount (about 23% more) of initiator solution was slowly poured into the clay dispersion while it was being stirred and ultrasonicated. The mixture was stirred and ultrasonicated for another 24 h. The resulting white precipitate was separated by filtration and then redissolved in deionized water. This filtration−dissolution process was repeated *10 times* in order to remove the free, unattached initiator. The final products were weighed after drying the precipitates in a vacuum oven at room temperature for 3 days, and the yield percentages were calculated. Table 1 summarizes the data concerning the preparation of the two types of intercalated clays. The yellowish powder product was stored in a desiccator for further characterization and subsequent SIP.

Polymerization with the Initiator-Intercalated Clay Particles. The initiator-intercalated clay was dissolved in THF solvent. The dispersion was ultrasonicated and vigorously stirred until a homogeneous system was observed (usually 6−10 h). Special care was taken to monitor the temperature to avoid premature decomposition of the AIBN-type initiator by adding ice to the sonication water bath. Styrene monomer was then added to the dispersion, and the mixture was stirred for 1 h under N_2 flow. Afterward, the temperature of a silicon oil bath was increased to 60 °C and the polymerization was held for 72 h under a N_2 atmosphere. As shown in Table 2, initiator and monomer concentration were kept constant for the two reactions so that the MWs of the two SIP products (mono-PS-M-2 is the product by the monocationic initiator and bi-PS-M-2 is the product by the bicationic initiator, where PS = polystyrene and M = montmorillonite) could be compared. Since the functionality of the two initiators is different, the ideal clay loading for their products is also different. The average yield of the SIPs was about 76%. Moreover, a pure polystyrene sample (PS-0) was synthesized as a reference using a recrystallized AIBN initiator under the same conditions.

Table 2. A Summary of Polymerization Results of Three Samples

product	initiator concn (10^3 mol/L)	monomer concn (mol/L)	ideal clay loading (wt %)[a]	M_n/PI[b] (free)	M_n/PI[b] (bound)
mono-PS-M-2	4.44	4.8	0.95	72K/2.15	51K/2.51
bi-PS-M-2	4.44	4.8	1.92	55K/2.13	16K/2.88
PS-0	4.44	4.8	N/A	124K/2.71	N/A

[a] Ideal clay loading: weight of clay/(weight of clay + weight of monomer). [b] Number-average molecular weight and polydispersity index: M_w/M_n by size exclusion chromatography (SEC).

SIP Product Separation. After the reaction, the solid product was dissolved in THF. The solution was then slowly poured into excess methanol. The resulting white precipitate (crude product) was filtered and dried for analysis and further separation. The crude powder product was redissolved in THF. The yellowish dispersion was centrifuged at 3000 rpm for 10 min. The supernatant liquid that contained free PS was separated by decantation. The centrifugation procedure was repeated five times by redissolving the remaining solid in THF. The free PS was recovered by adding the decanted solution to methanol. A counterion exchange process achieved the detachment of the electrostatically bound PS from the clay particles. The centrifuged PS-M product and excess LiBr were dissolved in THF. The mixture was stirred overnight. The resulting solution with yellowish precipitation was centrifuged. The bound polymer solution in THF was obtained by decantation for size exclusion chromatography MW analysis (Table 2).

Characterization and Instrumentation. *X-ray Diffraction (XRD).* XRD analysis of powder samples was performed on a Philips X'pert PW3040-MPD model diffractometer with a Cu Kα incident beam of wavelength 0.1543 nm. The Bragg equation was applied to calculate the *d* spacing of the clay platelets.

Thermogravimetric Analysis (TGA). All measurements were performed on a Mettler TGA50 model with a heating rate of 20 °C/min under N_2 flow. The samples were in the powder state and were dried in a vacuum oven at room temperature for at least 24 h to remove moisture before the measurements.

Infrared Spectroscopy (IR). Infrared spectra were obtained on a Nicolet NEXUS 470 FT-IR system. Powder samples were dispersed in methylene chloride, and drops of liquid were spread on a KBr plate. The IR spectra of bound polystyrene were measured by coating the decanted polymer solution on a KBr plate and evaporating THF. All sample disks were fully dried by air flow before analysis. All spectra were scanned 64 times with a resolution of 4 cm^{-1}.

X-ray Photoelectron Spectroscopy (XPS). Powder samples of pure and intercalated clays were analyzed by a Kratos Axis 165 Multi-technique Electron Spectrometer system. Powder samples were first pressed onto double-sided carbon tape before loading into the XPS analysis chamber. A nonmonochromatic Al Kα X-ray source (1486.6 eV) operated at 15 kV and 20 mA was applied to excite the photoelectron emission. Fixed analyzer transmission (FAT) mode was used, and survey scans (spot 800 × 200 μm^2, resolution of 4 eV at an analyzer pass energy of 160 eV) were collected from 0 to 1400 eV to obtain the elemental composition of the powder samples. The C 1s peak of the hydrocarbon signal (284.5 eV) was used as the binding energy reference. A built-in charge neutralizer was operated to compensate for charge buildup during the measurements.

Atomic Force Microscopy (AFM). The two SIP products (after removal of free polymer) were dispersed in toluene (1% w/w) and then spin-coated on silicon wafer pieces. A sample representing clay surfaces before SIP was prepared by placing a drop of homogenized clay suspension on a silicon wafer and evaporating the water. The clay particle morphologies before and after SIP were studied using a PicoScan system (Molecular Imaging) equipped with a 7 × 7 micron scanner. Magnetic AC (MAC) mode was used for all the AFM images. A MAC lever, a silicon nitride based cantilever coated with magnetic film, was used as the AFM tip. The force constant of the tip is 0.5 N/m, and the resonance

(16) Fan, X.; Park, M.-K.; Xia, C.; Advincula, R. *J. Mater. Res.* **2002**, *17*, 1622.
(17) Fan, X.; Locklin, J.; Youk, J. H.; Blanton, W.; Xia, C.; Advincula, R. *Chem. Mater.* **2002**, *14*, 2184.

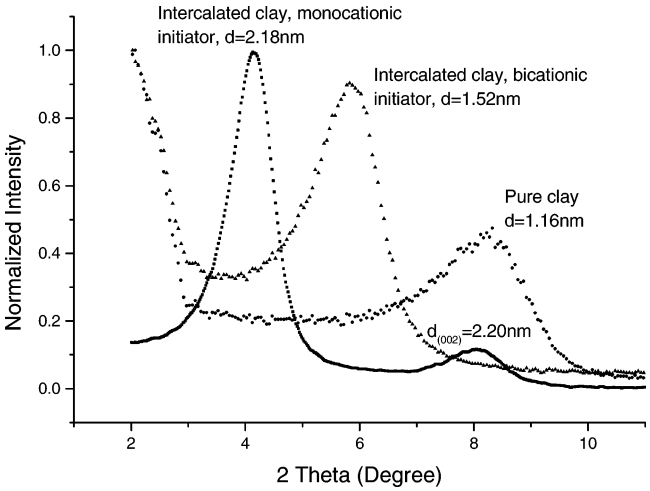

Figure 2. X-ray powder diffraction patterns of pure clay and two intercalated clay samples.

frequency is around 100 kHz. All samples were measured inside a suspension chamber to minimize ambient disturbance.

Size Exclusion Chromatography (SEC). With polystyrene standards, SEC was used to determine the MWs and polydispersity indices of free polystyrene formed in solution and polystyrene attached to clay surfaces.

Results and Discussion

Characterizations of Intercalated Clay Particles. X-ray powder diffraction patterns of the pristine clay and the two initiator-intercalated clay samples are shown in Figure 2. Some lamellar periodicity was maintained on the organophilic clays despite the rigorous sonication−centrifugation procedure to intercalate the initiators. By using the Bragg equation, $n\lambda = 2d \sin \theta$, the d spacing values of the samples were calculated and shown beside each peak.

The basal spacing of pure montmorillonite Na^+ is 1.16 nm, which is in accordance with data from other sources.[18] The XRD patterns of the intercalated clays indicate the successful insertion of the initiator molecules into the galleries of the silicate platelets since both intercalated clay samples gave increased d spacing values. Also, the sharper shape and the higher diffraction intensities of the peaks after intercalation provide more evidence in support of a better-ordered swollen structure than that of the original clay. This result demonstrates that the layered framework of inorganic clay can accommodate our AIBN derivative molecules of various functionalities with better long-range periodicity.

On further analysis, the d spacing values seemed to be inconsistent with the steric sizes of the two initiators. The d spacing of bicationic intercalated clay (1.52 nm) is much smaller than that of the monocationic intercalated clay although their molecular dimensions are about the same (both chain length values are 2.20 nm, estimated by Chem 3D software). We believe that the reason for this observation lies in the presence of charged groups on both ends of the bicationic initiator molecule. Thus, there are mainly two intercalation possibilities: (1) the two cationic endgroups interact electrostatically with two different but neighboring platelets' surfaces, or (2) they interact on the same side of a single clay particle. The combination of these two possibilities makes the intercalated structure less spatially ordered which could account for the significantly broadened reflection for this sample as compared with the peaks of the clay intercalated by the monocationic initiator. Furthermore, since XRD collects the average information from a large area of a powder sample, a synergic effect of these two possibilities accounts for an intermediate d spacing value. This interpretation is schematically shown in Figure 3. The interlamellar height shown in the figure is calculated by $\Delta d = d$ spacing − thickness of one platelet (∼1.0 nm).

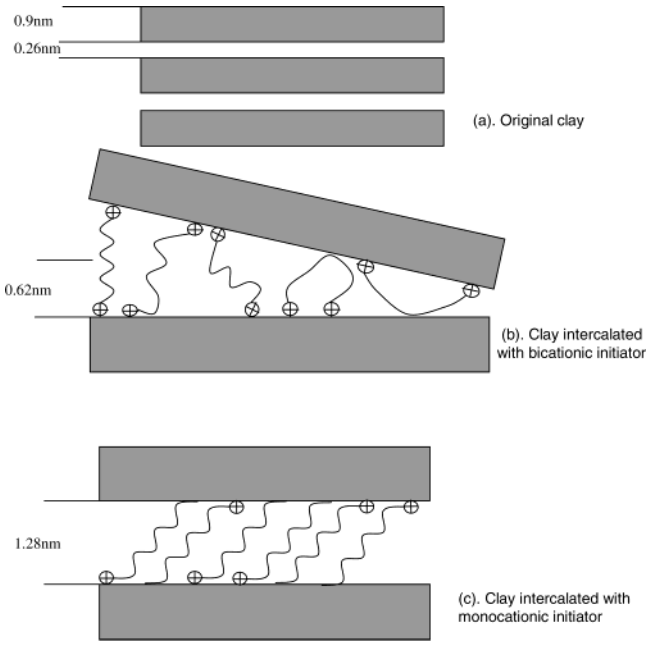

Figure 3. (a−c) Schematic diagrams of the intercalation: (a) original clay, (b) clay intercalated with bicationic initiator, and (c) clay intercalated with monocationic initiator.

In the case of the clay intercalated with monocationic initiator, the distance between two adjacent clay plates is 1.28 nm. A previous study showed a consistent 1.43 nm gallery height of the intercalated montmorillonite by a molecule with a $C_{18}H_{37}$ alkyl tail and a quaternized amine end.[19] Its chain length value was also estimated by Chem 3D software to be 2.41 nm (2.20 nm for our initiator), indicating the consistency of the results in terms of the intercalated molecular dimensions. Interestingly, for this intercalated clay, another small-intensity peak was observed at $2\theta = 8.1°$ besides the high-intensity peak at $2\theta = 4.1°$. There are also two possibilities for this secondary peak. (1) It might be a second-order diffraction peak from (002) planes, and the basal spacing is calculated to be 2.3 nm, which is very close to the value of its first-order diffraction peak. Similar higher order diffractions (up to third order) were also observed for intercalated smectite clays.[7] (2) Because the position of this peak approximately coincides with that of the peak of the pristine clay, it might also originate from the remaining, unswollen clay particles, which are not intercalated with the initiator. However, the second possibility could be ruled out by TGA and XPS results as explained later.

Figure 4 shows the TGA traces of pure clay, clay intercalated with bicationic initiator, and the pure initiator. As could be expected, the inorganic montmorillonite silicate shows very high thermal stability. The total weight loss is only 3.1%. This small percentage of weight loss is due to three different types of water present in the montmorillonite clay.[20] On the contrary, the organic initiator totally decomposes over the experimental tem-

(18) Kotov, N. A.; Haraszti, T.; Turi, L.; Zavala, G.; Geer, R. E.; Dekany, I.; Fendler, J. H. *J. Am. Chem. Soc.* **1997**, *119*, 6821.

(19) Vaia, R. A.; Teukolsky, K. R.; Giannelis, E. P. *Chem. Mater.* **1994**, *6*, 1017.

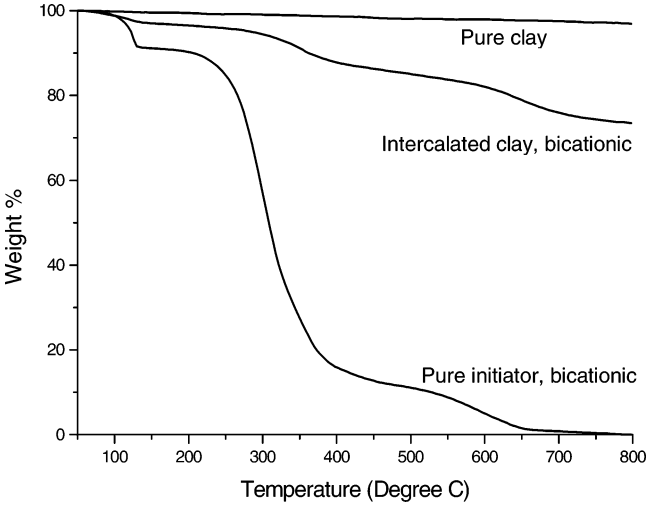

Figure 4. TGA traces of pure clay, clay intercalated with bicationic initiator, and pure bicationic initiator.

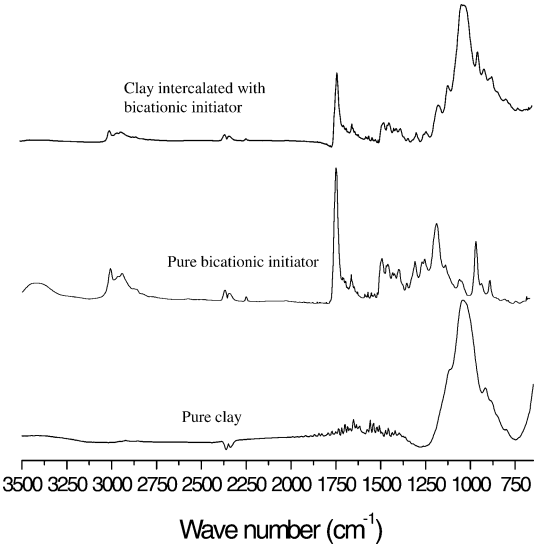

Figure 5. IR spectra of pure clay, pure bicationic free radical initiator, and intercalated clay.

perature range. Remarkably, for the pure initiator, there is a dramatic weight loss at about 120 °C, indicating decomposition of the azo group and the emission of N_2. Also for the intercalated clay, this decomposition occurs at the same temperature range and the overall degradation behavior is quite similar to that of the pure initiator, which indicates the presence of the initiator on clay particles.

The montmorillonite clay we used has a CEC value of 92 mequiv/100 g. According to this value, the ideal organic weight percentage of bicationic intercalated clay is calculated to be 17.5%. However, the corresponding TGA weight loss for the intercalated clay sample is 23.8% (total weight loss minus weight loss of pure clay), which is greater than the calculated value. One possibility for this difference is that the excessive amount of initiator added and the free unattached initiators were not washed away efficiently. However, the result indicates the completion of the cation exchange process, that is, all the replaceable Na^+ ions were exchanged with the initiator cations.

The same TGA measurements were performed on the samples related with the monocationic free radical initiator, and similar quantitative results were obtained. The calculated weight loss from the CEC value and the molecular weight of the initiator is 28.0%. The actual TGA weight loss is 30.1%. These data are consistent with each other and with those of the clays intercalated by the bicationic initiator. Thus, the same conclusions regarding the completion of the ion exchange process can be drawn. On the other hand, for both intercalated clay samples, a small portion of free, unattached initiator was not totally washed away. An excess amount of initiator was necessary in order to achieve a complete cation exchange and intercalation process in clay. Similar procedures for the total replacement of exchangeable cations on clay were also emphasized by other researchers.[9,21]

IR analysis further confirms the existence of the organic initiators on the intercalated clay samples. Figure 5 shows the IR spectra regarding the bicationic initiator and its intercalated clay samples. As expected, the IR spectrum of pure clay only shows strong absorbance at 1040 cm^{-1} due to the Si−O−Si bond in montmorillonite silicate. The spectrum of the pure initiators exhibits characteristic absorption peaks of C−H bonding at 2950−2800 cm^{-1}, the C═O carbonyl bond at 1734 cm^{-1}, and the C≡N nitrile bond at 2243 cm^{-1}. The above peaks in the spectra of pure silicate and pure initiator can be easily found in same wavenumber region in the spectra of intercalated clays. Although the IR absorbance for the intercalated clay sample is lower than that of the pure initiators, this still confirms the intercalation of the initiator into host clay galleries. It is also apparent that a synergic effect is observed from the three IR scans: the spectra of intercalated clays are superpositions of the pure clay and pure initiator spectra. Similar IR results were acquired from the samples associated with the monocationic initiator. Other studies have also demonstrated this synergic effect in polyaniline−montmorillonite clay and poly(ϵ-caprolactone)−fluorohectorite clay systems.[22,23]

The cation exchange process of sodium montmorillonite clay and charged initiator can be simply expressed by the following reaction:

$$Na^+\ clay^- + initiator^+\ Br^- \Rightarrow initiator^+\ clay^- + Na^+\ Br^-$$

If all the sodium ions are replaced by the initiator cation and the product is thoroughly washed, there should be no sodium ions remaining in the intercalated clays. By using XPS, the completion of the above ion exchange reaction was further confirmed.

Figure 6 shows the XPS survey scan spectra of the pure and intercalated clay samples. As labeled in spectrum a, characteristic peaks of O, Si, Al, and Mg are clear for the pristine montmorillonite clay, which is chemically a magnesium aluminum silicate. Besides these signals from the clay, spectra b and c also show C 1s and N 1s peaks, again demonstrating the presence of the organic initiator molecules on the clay. However, the most important result from XPS analysis is the change in the Na signal before and after the ion exchange reaction. In scan a, the photoelectron line of Na 1s (1072 eV) and the Auger line of Na KLL (493 eV) are very obvious, indicating that the clay's counterion is the Na^+ cation. After cation exchange, those two characteristic emissions for sodium disappear for both intercalated clay samples. Thus, other than the

(20) Xie, W.; Gao, Z.; Pan, W.; Hunter, D.; Vaia, R. A.; Singh, A. *PMSE Prepr.* **2000**, *82*, 284.
(21) Fan, X.; Xia, C.; Christofoli, W.; Zhou, Q.; Mays, J.; Advincula, R. *Polymer Prepr.* (*Am. Chem. Soc., Div. Polym. Chem.*) **2002**, *43*, 683.
(22) Choi, J.; Kim, W.; Kim, G.; Kim, H.; Joo, J. *PMSE Prepr.* **2000**, *82*, 245.
(23) Messersmith, P.; Giannelis, P. *Chem. Mater.* **1993**, *5*, 1064.

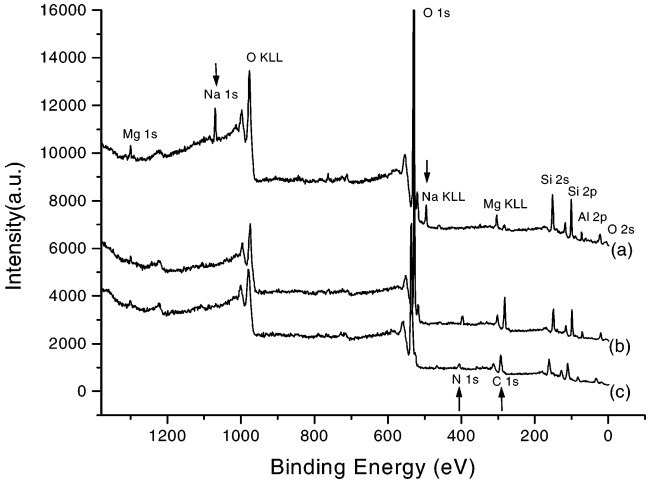

Figure 6. XPS spectra of pure clay and two intercalated clays: (a) pure clay, (b) clay intercalated with the monocationic initiator, and (c) clay intercalated with the bicationic initiator.

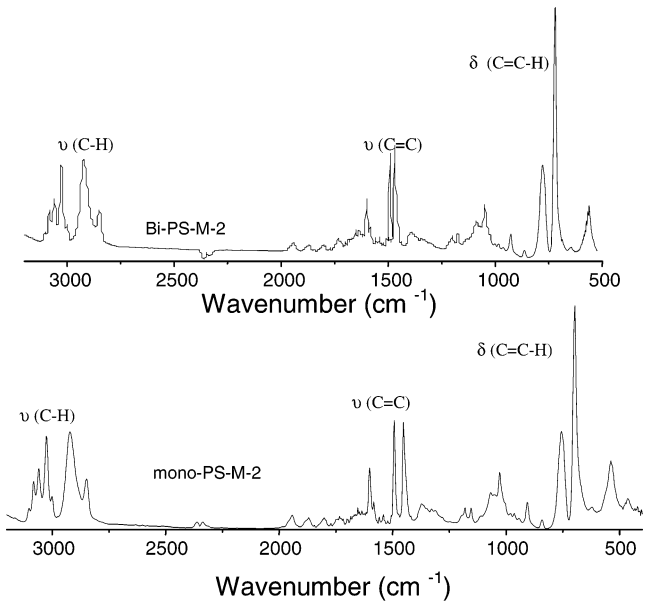

Figure 7. IR spectra of 2 bound polymers (polystyrene) after removal from clay particles.

results from TGA, this is additional convincing evidence supporting our conclusion of the complete cation exchange process. Moreover, it is clear that the second XRD peak previously shown should be the second-order diffraction of totally swollen clay lamellae, rather than a peak from a remaining small portion of unintercalated clay particles.

Characterization of SIP Nanocomposite Products. Successful preparation of the organophilic clay can facilitate free radical SIP because it provides initiation functionalities for polymerization. In addition, it improves the homogeneity of the intercalated clay−monomer−solvent mixture to achieve an efficient polymerization system. The results are as follows:

First, IR spectroscopy confirmed the presence of polystyrene on clay for both SIP reactions. As labeled in Figure 7, for both bound polymer samples, the vibrational bands typical for polystyrene, such as C−H aromatic and aliphatic stretching at 3100−2800 cm^{-1}, C═C vibrations at 1600, 1550, and 1458 cm^{-1}, and strong C−H out-of-plane bendings at 698 and 758 cm^{-1}, are observed.

As shown in Table 2, although the initiator concentration was kept constant, the MWs of free polymer and bound polymer of the three samples are quite different. Free

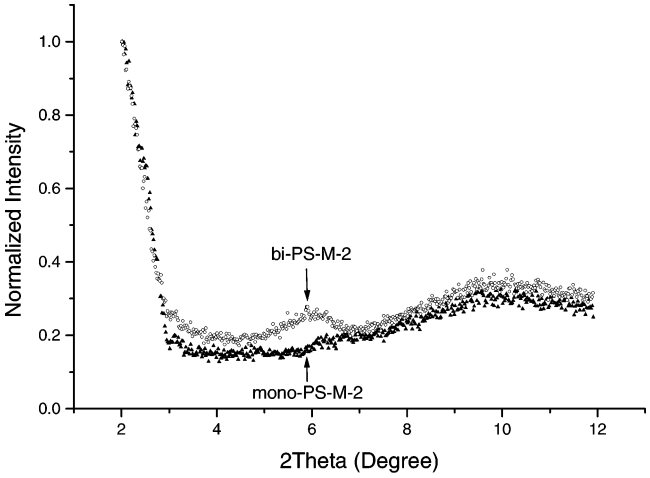

Figure 8. XRD spectra of the two SIP nanocomposites showing degree of exfoliation.

polymer comes from the free initiators that are not washed away during the intercalation procedure. In the case of clay intercalated with monocationic initiator, it can also originate from the free end (two radicals are generated upon the decomposition of the azo group) that is not ionically bound to the clay surface. Table 2 shows that both SIP samples have a lower free polymer MW than the control. Also sample bi-PS-M-2, which has a higher clay loading, gives a lower molecular weight. The presence of clay particles in the polymerization system definitely affects the mechanism of free polymer chain growth. The possible reason is that clay platelets act as barriers blocking free radical chains from growing. This can be accounted for in two cases: (1) A growing chain from a clay platelet interface and surface has slower monomer diffusion kinetics compared to a more homogeneous free solution system. The initiator density and the polymer chain growth mechanism from a surface play an important role. (2) The radical chain end of free polymer is more likely to react with the nearby ionically immobilized polymers and initiators on the clay platelet or the perimeter of clay particle stacks. Thus, rather than monomer addition, a higher probability of free radical termination or transfer is induced, resulting in a lower MW than that of the reference sample. In addition, aluminosilicate clays have been previously reported to act as inhibitors for free radical polymerization, where the propagating radicals could be terminated by absorption to Lewis acid sites on the clay surface.[24] Lower MW and higher polydispersity were reported for poly(methyl methacrylate) (PMMA)−clay nanocomposites polymerized with higher clay content as supported by SEC and NMR studies by Venables et al.[25]

In terms of bound polymer, mono-PS-M-2 has a much higher MW (51K) than that of bi-PS-M-2 (16K), indicating SIP is more successful with the monocationic initiator. One of the reasons is that the initiated-clay particles can be more easily dispersed in polymerization solution than the bicationic counterpart, rendering the surface-attached initiators greater accessibility to monomer addition. This explanation will be more clear after discussing the XRD structural analysis of the two SIP products.

The X-ray diffractograms of the two SIP products are shown in Figure 8. The broad peaks of both samples at the higher angle regime are believed to be related to the

(24) Solomon, D. H.; Swift, J. D. *J. Appl. Polym. Sci.* **1967**, *11*, 2567.
(25) Tabtiang, A.; Lumlong, S.; Venables, R. A. *Eur. Polym. J.* **2000**, *36*, 2559.

long-range order of the polystyrene matrix. Similar broad peaks were also observed in the diffractogram of the PS-0 reference sample (not shown) and polystyrene−clay nanocomposite material by another SIP approach.[9] Sample bi-PS-M-2 shows a small peak at $2\theta = 5.9°$, which is about the same as the peak position of the corresponding intercalated clay (Figure 2). This result indicates that this product still contains intercalated clay structure. On the contrary, there is no peak on the XRD trace of sample mono-PS-M-2, indicating a completely exfoliated structure was achieved in this sample.

This result was unexpected. We assumed that for the clay/bicationic initiator system, adjacent clay layers would be gradually pushed apart during SIP, once the two immobilized free radicals were simultaneously generated. As a result, the intercalated clay stacks would be totally delaminated, forming a fully exfoliated nanocomposite product. However, polymer can only grow within the clay gallery when monomer effectively diffuses into the tethered radicals within the interlayer spacing. The time scale of diffusion is such that access to the monomer from within the layers is limited. Considering the rapid kinetics for free radical polymerization in solution, this intercalative monomer diffusion is much slower toward monomer addition. Thus, free initiators exhaust the monomers while SIP inside clay lamellae is delayed by diffusion. Furthermore, there is also competition from the surface-perimeter-attached initiators of the clay particles. From the combination of XRD peak position (Figure 8), low molecular weight, and higher polydispersity (Table 2), we believe that most of the polymer obtained (after degrafting) is the result of chain initiation and growth from initiators attached to the nanoparticle perimeter rather than the clay intergallery spaces. This explanation is consistent with bi-PS-M-2 retaining some intercalated structure. Even if some of the bicationic initiators were activated and grew to become oligomers, the growing chains will likely be terminated by recombination or disproportionation by nearby immobilized growing chains/initiators in the same gallery. Hence the low molecular weight and high polydispersity of bi-PS-M-2 can be explained.

By comparison, the intercalated monocationic initiator is more easily delaminated than the bicationic initiator. The monocationic initiator molecule is also more organophilic. The weaker van der Waals interaction between the alkyl headgroups of the monocationic initiator and clay surfaces makes the intercalated clay more easily swelled by the solvent and monomer. Once the clay intercalated with monocationic initiator is exfoliated by sonicating and stirring, the attached initiators have more accessibility to monomer, that is, better monomer intercalative diffusion.

On the other hand, neighboring clay platelets are electrostatically bound by the two charged ends in the case of the bicationic initiator (Figure 3). It is more difficult to delaminate clay stacks that are ionically held together. Thus, SIP of mono-PS-M-2 is much more successful than that of bi-PS-M-2. This explanation is supported by the higher molecular weight of its free polymer (Table 2) and the exfoliated structure of the product. Fu and Qutubuddin recently prepared a polystyrene−clay nanocomposite with an exfoliated structure through a different strategy.[26] In their studies, montmorillonite clay was first intercalated by a cationic surfactant (vinylbenzyldimethyldodecylammonium chloride, VDAC) and then dispersed in styrene monomer followed by polymerization with AIBN initiator. Nevertheless, the solubility of VDAC in the monomer and the importance of well dispersing the organophilic clay in the monomer were stressed. Also, a "vortex and sonication for 4 h" process was used to prepare a well-dispersed intercalated clay. In our recent attempt for LASIP of styrene from clay surfaces, we also concluded that a key factor for successful SIP is to disperse intercalated clay more efficiently in the solvent in order to make the monomer more accessible to active anionic sites.[10,11] Recent results by Brittain et al. highlighted the use of suspension and emulsion polymerization to prepare PMMA−clay nanocomposites from three OLS clays modified by an ammonium salt with a long alkyl chain, AIBA initiator, and a cationic methacrylate comonomer.[27] Similarly, Lee et al. recently reported bulk polymerization of organophilic clay modified by a polymerizable methacrylate surfactant that had a long alkyl chain.[28] While different degrees of intercalation and exfoliation were found in their nanocomposites, those studies *emphasized* the importance of tethering polymer chains to clay surfaces toward the exfoliated structure. Although the free radical method was used in both works, a significant difference with our SIP approach is that of direct and complete attachment of polymerization initiators on partially exfoliated clay nanoparticles, resulting in polymer shell coated clay nanoparticles.

AFM observations of clay nanoparticle morphology (Figure 9a−c) further justify our comparison between the two types of initiators. The platy shape and sharp edge profile of the original montmorillonite clay nanoparticles are readily observed. After SIP, the morphology of clay particles was significantly different. As shown in Figure 9b, clay platelets in bi-PS-M-2 mostly exist in the form of aggregates, indicating the structure of this composite material is still intercalated. On the contrary, clay platelets in mono-PS-M-2 are mostly discrete particles (Figure 9c), indicating the highly exfoliated structure of this sample. Moreover, the round shape and smooth edge of the exfoliated particles indicate the "wrapping" of bound polymer to form a shell. In contrast, the sharp particle edge of the clay aggregates of bi-PS-M-2 is still discernible; demonstrating the free radical SIP through the bicationic initiator was less successful. Note that unlike rigid Laponite synthetic clays, montmorillonite platelets are easily deformed and broken (brittle). This is evident in the different size and size distribution between the original and SIP clay particles, brought about by the extensive sonication and centrifugation process used to isolate the particle samples. In summary, these AFM results are consistent with the analysis of the MW, IR, X-ray, and XPS data of the samples as previously discussed.

Conclusions

Mono- and bicationic free radical initiators were synthesized and intercalated into montmorillonite clay nanoparticle surfaces for free radical SIP of styrene. The properties of the two intercalated clays and SIP products were comparatively analyzed by a series of characterization methods. XRD results showed that the clay intercalated with monocationic initiator has a larger *d* spacing and more ordered structure. IR, XPS, and qualitative TGA confirmed the attachment of both initiators. Complete cation exchange was confirmed by quantitative TGA and XPS. XRD further showed that the SIP product of the bicationic initiator retained some intercalated structure while a completely exfoliated structure is achieved through the monocationic initiator. We have found that efficient

(26) Fu, X.; Qutubuddin, S. *Mater. Lett.* **2000**, *42*, 12.

(27) Huang, X.; Brittain, W. J. *Macromolecules* **2001**, *34*, 3255.
(28) Zeng, C.; Lee, L. J. *Macromolecules* **2001**, *34*, 4098.

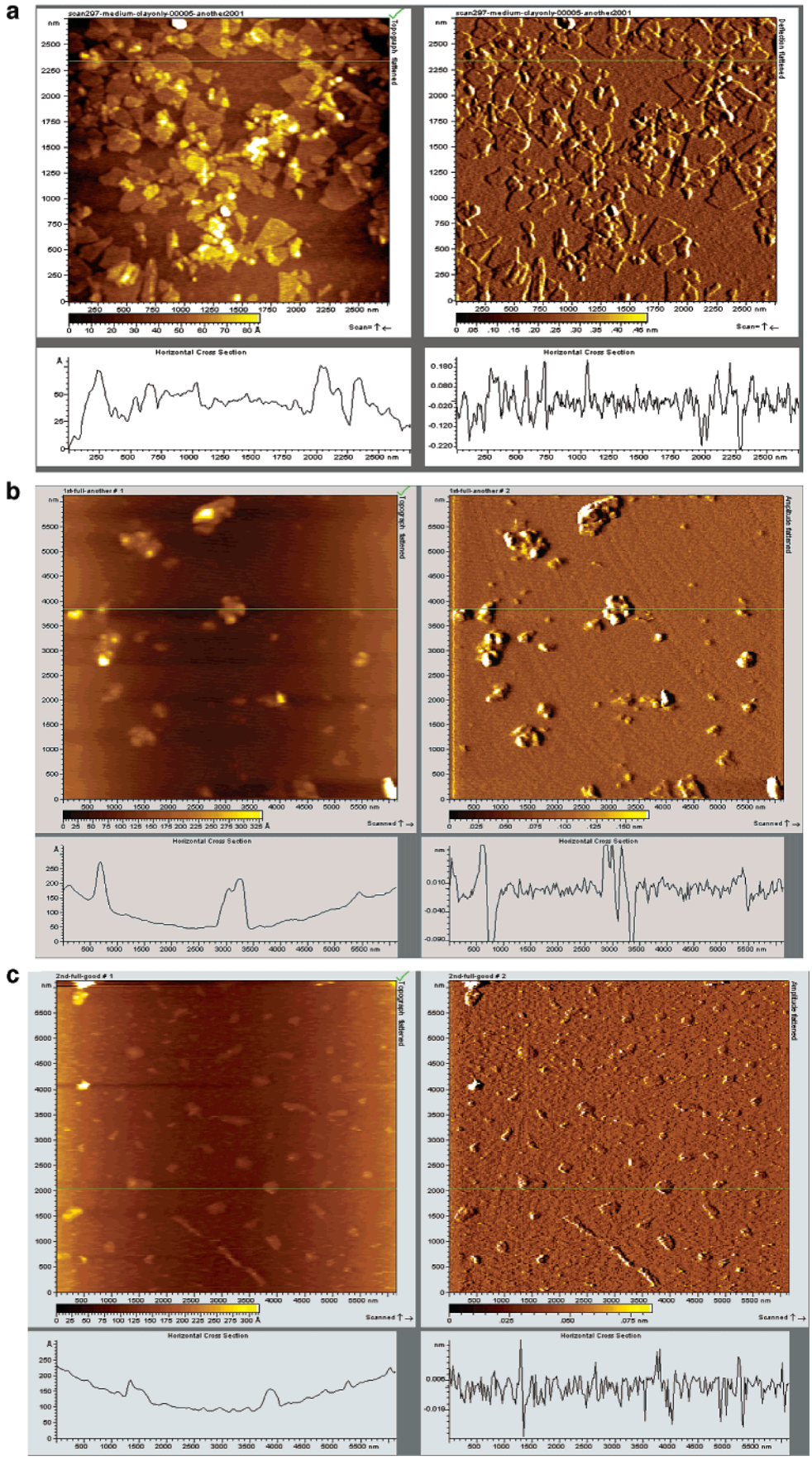

Figure 9. (a−c) AFM pictures of (a) the original clay, (b) bi-PS-M-2 after removal of free polymer, and (c) mono-PS-M-2 after removal of free polymer. Note the differences in scale between the images.

nanoparticle dispersion and monomer diffusion are crucial factors in performing a successful SIP and in achieving complete exfoliated clay structures. This will require further experiments to correlate diffusion coefficients with various clay structures and dispersion methods. SEC showed that the SIP product of the monocationic initiator has a higher MW for both free and bound polymer. Finally, in correlation with the observed nanoparticle morphologies by AFM, we conclude that SIP on clay nanoparticles is more successful through the use of a monocationic initiator.

Acknowledgment. This project was supported by the Army Research Office (Grant Number DAAD-19-99-1-0106). Montmorillonite clay (commercially Cloisite Na^+) was generously provided by Southern Clay Products, Gonzales, Texas. We also appreciate Dr. Yogesh Vohra, Dr. Shane Cetledge, Dr. Juan Pablo Claude, and John Kestell at the University of Alabama at Birmingham for their help on XRD and IR analysis. We also acknowledge Dr. Earl Ada of the University of Alabama—Tuscaloosa for the XPS measurements.

Supporting Information Available: Synthesis procedure and results (NMR data) for the monocationic and bicationic initiators. This material is available free of charge via the Internet at http://pubs.acs.org.

LA0268193